

## Transit Time Effect in High-Frequency Characteristics of HBTs

Seonghearn Lee and Anand Gopinath

Department of Electrical Engineering, University of Minnesota  
200 Union Street S.E., Minneapolis, MN 55455

**Abstract** - We present simulation results that show negative output resistance may exist at frequencies beyond  $f_{max}$  in the conventional mesa emitter-up AlGaAs/GaAs heterojunction bipolar transistors. It is shown that larger collector transit time is preferable choice to increasing base transit time in the design of this structure.

### Introduction

Dagli et al. [1] have shown that negative output resistance may be obtained in emitter-down heterojunction bipolar transistor (HBT), as a result of transit time phase delay in the common-base current gain. To obtain this negative output resistance, the parasitics of HBTs should be small. In this paper, we investigate the transit time effect of mesa etched emitter-up type HBT structure using the small signal equivalent circuit model and demonstrate that, with a thin heavily doped base (0.05  $\mu\text{m}$ ) together with a collector (0.65  $\mu\text{m}$ ), negative output resistance may occur at frequencies well above  $f_{max}$ . All circuit model parameters are related to layer and layout parameters, by using resistance and capacitance models, together with empirical mobilities and contact resistivities to obtain realistic estimates of the transit time and parasitics.

### High-Frequency Small-Signal Circuit Model

The schematic diagram for AlGaAs/GaAs HBT is shown in Fig. 1. Table I shows the layout and layer structure parameters used in our simulations. In the equivalent circuit model shown in Fig. 2,  $C_e$  is the emitter-base junction and diffusion capacitance,  $C_c$  is the intrinsic base-collector junction capacitance,  $C_{bc}$  is the extrinsic base-collector junction capacitance,  $r_e$  is the dynamic emitter resistance,  $r_b$  is the intrinsic base resistance,  $r_{cc}$  is the collector resistance,  $r_{ee}$  is the emitter resistance, and  $r_{bp}$  is the base contact resistance. The values of all parameters are calculated by resistance and capacitance models [2], [3] with empirical mobilities and lifetime [4], [5] and contact resistivities [6]. The size of the device for these simulations was chosen to be  $1 \times 4 \mu\text{m}^2$  for the emitter.

The most important parameter in this simulation is the transit time-dependent common-base current gain expressed as [7]

$$\alpha = \alpha_0 \left[ \frac{e^{-j\omega(\tau_c + (m/\omega_\alpha))}}{1 + j(\omega/\omega_\alpha)} \right] \quad (1)$$

$$\text{where } \tau_c = \frac{X_{dc}}{2v_{sat}}, \quad \omega_\alpha = \frac{2.4 D_{nb}}{W_b^2}$$

where  $\alpha_0$  is the dc value of the current gain,  $\omega_\alpha$  is the  $\alpha$  cutoff frequency for the compositionally ungraded and uniformly doped base,  $\tau_c$  is the collector transit time,  $X_{dc}$  is the collector-base depletion layer width,  $v_{sat}$  is the electron saturation velocity,  $D_{nb}$  is the minority electron diffusion constant in p-type GaAs base, and  $m$  is the excess phase shift due to the drift-diffusion mechanism of carrier transport in the base and is equal to 0.22 for a uniformly doped base.

$\alpha_0$  is calculated by assuming the perfect emitter injection efficiency.

$$\alpha_0 = \operatorname{sech} \left( \frac{W_b}{L_{nb}} \right)$$

where  $L_{nb}$  is diffusion length for minority electron in the base and is given by

$$L_{nb} = \sqrt{D_{nb} \tau_{nb}}$$

where  $\tau_{nb}$  is the minority electron lifetime in the base, and  $D_{nb}$  is obtained by Einstein relation,  $D_{nb} = (kT/q) \mu_n p$ .

### Output Resistance Calculations

The h-parameters are calculated from the small signal equivalent circuit model shown in Fig. 2, and from this the output resistance is calculated by

$$r_{22} = \operatorname{Re}(1/h_{22})$$

The effect of base and collector transit times on the frequency response of the output resistance is shown in Fig. 3. The base width ( $W_b$ ) is used as the main parameter for controlling the base transit time, and the collector width ( $W_c$ ), for the collector transit time. The curves in this figure are for following parameters: curve 1:  $W_b = 0.05 \mu\text{m}$ ,  $W_c = 0.65 \mu\text{m}$ ; curve 2:  $W_b = 0.40 \mu\text{m}$ ,  $W_c = 0.65 \mu\text{m}$ ; curve 3:  $W_b = 0.05 \mu\text{m}$ ,  $W_c = 2.00 \mu\text{m}$ . For base-collector junction,  $V_{BC} = -1 \text{ V}$  is used for curves 1 and 2, and  $V_{BC} = -13 \text{ V}$  is used for curve 3 to ensure full depletion of collector. From Equation (1), if we define the base transit time as  $\tau_b = 1/\omega_\alpha$  for convenience, the transit times at the saturation velocity of  $10^7 \text{ cm/s}$  are approximated by  $\tau_b = 0.4 \text{ ps}$ ,  $\tau_c = 3.3 \text{ ps}$  for curve 1,  $\tau_b = 24.7 \text{ ps}$ ,  $\tau_c = 3.3 \text{ ps}$  for curve 2, and  $\tau_b = 0.4 \text{ ps}$ ,  $\tau_c = 10.0 \text{ ps}$  for curve 3.

As shown in Fig. 3, the dependence of output resistance on the frequency has a different profile in curve 2 and 3 when compared to curve 1. Positive output resistance at low frequencies for curves 2 and 3 is about 9 times larger than that for curve 1. Negative resistance regions are induced by the phase delay due to the transit time. Note that curve 3 has a larger magnitude of negative resistance than that of curves 1 and 2, and the frequency band of curve 2 has a similar value of negative resistance as curve 1. From Fig. 3, the maximum magnitudes of negative resistance are  $57 \Omega$  for curve 1,  $49 \Omega$

IF1

for curve 2, and  $1435 \Omega$  for curve 3. Thus, increasing the collector transit time obtains large values of negative output resistance. This negative resistance may be used in oscillators, and three terminal devices with negative output resistance are superior to two terminal negative resistance devices like IMPATT diodes, because of the isolation between input and output. The frequencies of the negative resistance bands are important in oscillator applications. The first frequency band of negative resistance is shifted to lower frequency region as transit time increases. This is clearly demonstrated by comparing curve 1 with curves 2 and 3 in Fig. 3.

### Conclusions

Multiple negative resistance bands are predicted at frequencies beyond  $f_{max}$  in the conventional mesa type emitter-up AlGaAs/GaAs HBTs with careful design and reduced parasitics. Thus, HBT power gain may be obtained in these frequency bands with the negative resistance even above  $f_{max}$ . To obtain the usable transit time effect with large negative resistance, the increase of collector transit time is preferable to increasing base transit time. Therefore, for transit time HBTs, the base should be designed to be as thin as possible, and collector should be thick enough to obtain the large transit time at the frequency range of interest, while keeping parasitics small.

### References

- [1] N. Dagli, W. Lee, S. Prasad, and C.G. Fonstad, "High-frequency characteristics of inverted-mode heterojunction bipolar transistors," *IEEE Electron Device Lett.*, vol. 8, p. 472-474, 1987.
- [2] M. B. Das, "High-frequency performance limitations of millimeter wave heterojunction bipolar transistors," *IEEE Trans. Electron Devices*, vol. 35, p. 604-614, 1988
- [3] D. A. Sunderland and P. D. Dapkus, "Optimizing n-p-n and p-n-p heterojunction bipolar transistors for speed," *IEEE Trans. Electron Devices*, vol. 34, no. 2, p. 367, 1987.
- [4] M. S. Lundstrom et al., "Physics and modeling of heterostructure semiconductor devices," *SRC Tech. Rep.* 079, 1984.
- [5] S. Tiwari and S. L. Wright, "Material properties of p-type GaAs at large dopings," *Appl. Phys. Lett.* vol. 56, no. 6, p. 563, 1990.
- [6] M. Shur, *GaAs devices and circuits*, Plenum, New York, 1987, p. 149-152.
- [7] K. C. Gupta, R. Garg, and R. Chadha, *Computer-aided design of microwave circuits*, Artech House, MA, 1981, p. 270-273.

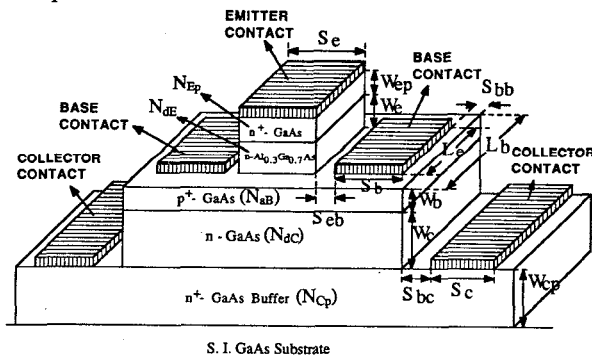


Fig. 1. The schematic diagram for simulated AlGaAs/GaAs HBT.

|          |                    |          |                                    |
|----------|--------------------|----------|------------------------------------|
| $W_e$    | $0.15 \mu\text{m}$ | $S_{bb}$ | $0.5 \mu\text{m}$                  |
| $W_b$    | Variable           | $S_{bc}$ | $5.0 \mu\text{m}$                  |
| $W_c$    | Variable           | $S_c$    | $5.0 \mu\text{m}$                  |
| $W_{ep}$ | $0.2 \mu\text{m}$  | $N_{DE}$ | $1 \times 10^{17} \text{ cm}^{-3}$ |
| $W_{cp}$ | $1.0 \mu\text{m}$  | $N_{AB}$ | $1 \times 10^{19} \text{ cm}^{-3}$ |
| $L_e$    | $4.0 \mu\text{m}$  | $N_{DC}$ | $5 \times 10^{15} \text{ cm}^{-3}$ |
| $L_b$    | $5.0 \mu\text{m}$  | $N_{EP}$ | $6 \times 10^{18} \text{ cm}^{-3}$ |
| $L_c$    | $15.0 \mu\text{m}$ | $N_{CP}$ | $6 \times 10^{18} \text{ cm}^{-3}$ |
| $S_e$    | $1.0 \mu\text{m}$  | $J_c$    | $8000 \text{ A/cm}^2$              |
| $S_{eb}$ | $0.35 \mu\text{m}$ | $V_{BC}$ | Variable                           |
| $S_b$    | $1.5 \mu\text{m}$  |          |                                    |

Table I. Layout and layer structure parameters used in our calculations.

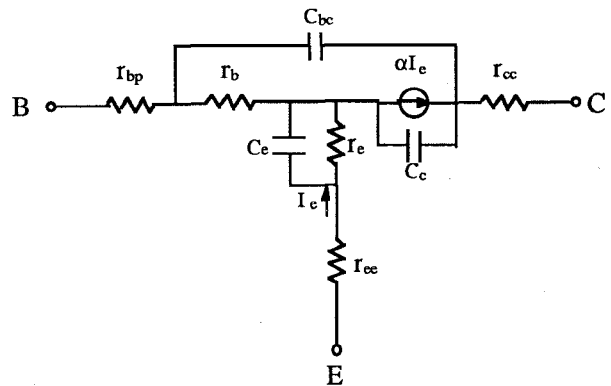


Fig. 2. High frequency equivalent circuit model for simulated AlGaAs/GaAs HBT.

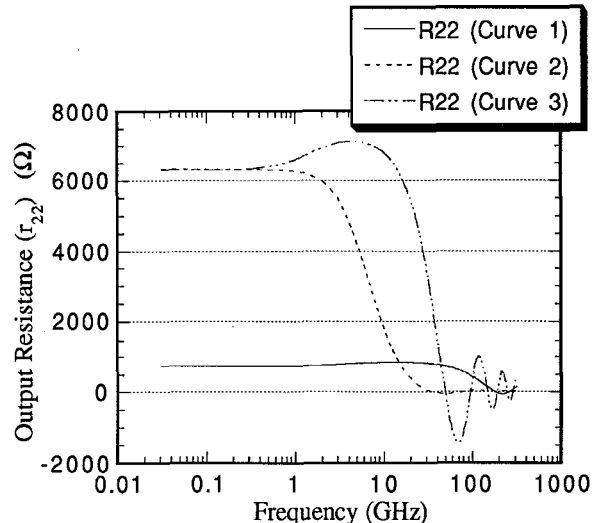


Fig. 3. The small-signal output resistance  $r_{22}$  as a function of frequency.